CHAPTER NINE

Methods for Cell and Particle Tracking

Erik Meijering, Oleh Dzyubachyk, *and* Ihor Smal

Contents

Abstract

Achieving complete understanding of any living thing inevitably requires thorough analysis of both its anatomic and dynamic properties. Live-cell imaging experiments carried out to this end often produce massive amounts of time-lapse image data containing far more information than can be digested by a human observer. Computerized image analysis offers the potential to take full advantage of available data in an efficient and reproducible manner. A recurring task in many experiments is the tracking of large numbers of cells or particles and the analysis of their (morpho)dynamic behavior. In the past decade, many methods have been developed for this purpose, and software tools based on

Biomedical Imaging Group Rotterdam, Departments of Medical Informatics and Radiology, Erasmus MC—University Medical Center Rotterdam, Rotterdam, The Netherlands

Methods in Enzymology, Volume 504
ISSN 0076-6879, DOI: 10.1016/B978-0-12-391857-4.00009-4

these are increasingly becoming available. Here, we survey the latest developments in this area and discuss the various computational approaches, software tools, and quantitative measures for tracking and motion analysis of cells and particles in time-lapse microscopy images.

1. Introduction

A fundamental property of any real-world object is that it extends in both space and time. This is particularly true for living organisms, which, by definition, require the passage of time for their metabolism, growth, reaction to stimuli, and reproduction. Full understanding of any animate entity therefore necessitates studying not only its spatial (anatomic) but also its temporal (dynamic) properties (Tsien, 2003). It is therefore no surprise that research in medicine and biology has come to rely increasingly on time-lapse imaging and longitudinal examinations. In both the health sciences and the life sciences, the technologically deficient times when researchers had to draw conclusions based on static two-dimensional (2D) images are long gone, and it is now commonplace to image and study subjects in three dimensions over time (denoted 3D + t or 4D).

Live imaging of dynamic processes at the cellular and molecular levels has been made possible by the development of a vast spectrum of fluorescent proteins and nanocrystals and groundbreaking advances in optical microscopy technology. The resulting increase in the amount, size, dimensionality, and complexity of the image data has brought about new challenges for automated data analysis and management (Peng, 2008; Rittscher, 2010; Swedlow *et al.*, 2009; Vonesch *et al.*, 2006). A topic for which interest has increased exponentially in recent years (Fig. 9.1) is object tracking (Dorn *et al.*, 2008; Jaqaman and Danuser, 2009; Meijering *et al.*, 2006, 2009; Rohr *et al.*, 2010; Zimmer *et al.*, 2006). Indeed, it is practically impossible to manually follow hundreds to thousands of cells or particles through many hundreds to thousands of image frames, and sophisticated computerized methods are very much needed for these tasks.

Although first attempts to automate the tracking of cells or particles by digital image processing date back at least 30 years, the development of more advanced tracking methods really took off in the past decade, and it is only since a couple of years that biology at large is able to reap the fruits of these efforts through the increased availability of software implementations of such methods. The purpose of this chapter is to summarize these developments and to provide hands-on suggestions for practitioners in the field. After a brief description of the main tracking approaches, we highlight freely

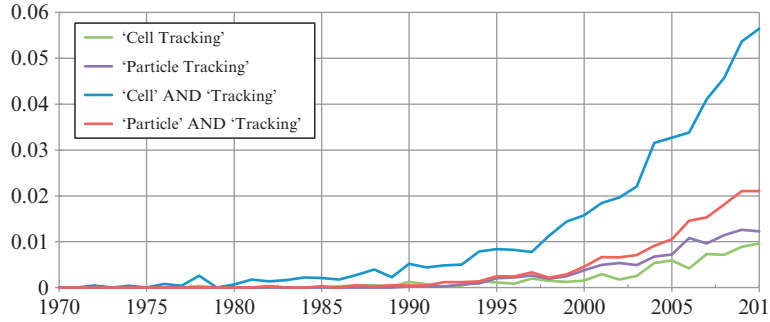

Figure 9.1 Percentage of publications in the PubMed database (National Library of Medicine, National Institutes of Health, Bethesda, MD, USA) as a function of publication year for the indicated combinations of words in the title and/or abstract. The plot shows the exponentially increasing interest in cell and particle tracking in the biomedical (and related) literature. Notice that by plotting percentages (of the total body of literature published in any given year), we have corrected for the intrinsic growth of the number of publications. In other words, the curves indicate a rising "market share" of tracking-related research.

available software tools for cell and particle tracking, discuss frequently used measures to quantify dynamics, and conclude with concrete tips and tricks on various practical aspects.

2. Tracking Approaches

Before discussing tracking tools, it is useful to survey the different methodological approaches on which these may be based. Since the appearance and behavior of cells can be quite different from particles, the image processing techniques developed to track them are usually also quite different and are therefore discussed separately here. In either case, there are generally two sides to the tracking problem: (1) the recognition of relevant objects and their separation from the background in every frame (the segmentation step) and (2) the association of segmented objects from frame to frame and making connections (the linking step).

2.1. Cell tracking approaches

In images where the cells have sufficiently and consistently different intensities than their surroundings, they are most easily segmented by thresholding, which labels pixels above the intensity threshold as "object" and the remainder as "background", after which disconnected regions can be automatically

labeled as different cells. In the case of severe noise, autofluorescence, photobleaching (in fluorescence microscopy), very poor contrast, gradients, or halo artifacts (in phase-contrast or differential interference contrast microscopy), thresholding will fail, and more sophisticated segmentation approaches are needed. Popular examples (see Meijering *et al.*, 2008, 2009 for a more elaborate discussion) are template matching (which fits predetermined patches or models to the image data but is robust only if cells have very similar shape), watershed transformation (which completely separates images into regions and delimiting contours but may easily lead to oversegmentation), and deformable models (which exploit both image information and prior shape information).

The simplest approach to solving the subsequent association problem is to link every segmented cell in any given frame to the nearest cell in the next frame, where "nearest" may refer not only to spatial distance but also to difference in intensity, volume, orientation, and other features. This nearest-neighbor solution works well as long as the cells are well separated in at least one of the dimensions of the feature space. Essentially, this criterion also applies to so-called online cell tracking approaches, which alternate between segmentation and linking on a per-frame basis. For instance, template matching, mean-shift processing, or deformable model fitting is applied to one frame, and the found positions or contours are used to initialize the segmentation process in the next frame, and so on, which implicitly solves the linking problem (see Fig. 9.2 for an example result of applying such a scheme to a challenging tracking problem).

2.2. Particle tracking approaches

Individual proteins or other (macro)molecular complexes within cells (collectively referred to as particles) are hardly (if at all) visible in bright field or phase-contrast microscopy and require fluorescent labeling and imaging. Since fluorescent proteins are two orders of magnitude smaller (nanometer range) than the optical resolution of typical microscopes (100 nm or worse), they appear as diffraction-limited spots (foci) in the images. If their contrast to the background is sufficiently large throughout the image, they can be localized to nanometer resolution by intensity thresholding and computing the centroid position of each segmented spot or by fitting a theoretical or experimentally acquired model of the point spread function (Carter *et al.*, 2005; Cheezum *et al.*, 2001). However, in live-cell imaging, the contrast is often poor, and more sophisticated approaches are needed. The results of a recent comparison study (Smal *et al.*, 2010) suggest that better results can be obtained by specialized algorithms from mathematical morphology and supervised (machine-learning) approaches.

Similar to cell tracking, the most straightforward strategy to solve the association problem is to apply local nearest-neighbor linking. However,

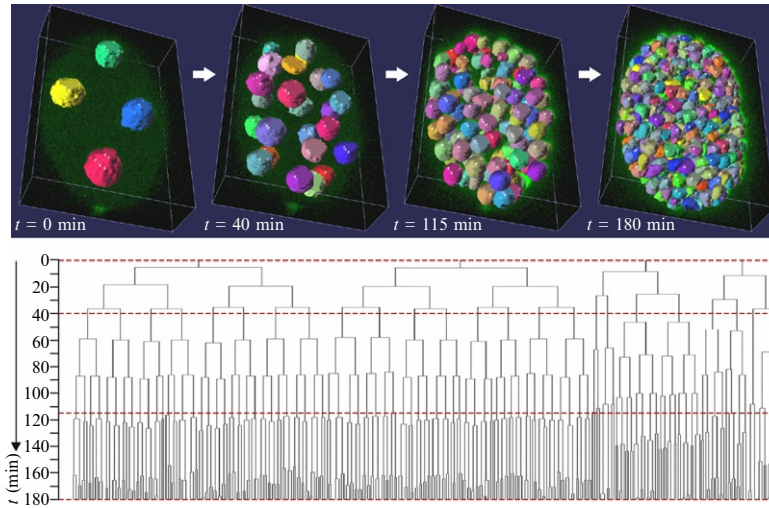

Figure 9.2 Cell tracking and lineage reconstruction for studying embryogenesis. The top row shows four time points of a 3D + *t* fluorescence microscopy image data set of a developing *Caenorhabditis elegans* embryo, starting from the 4-cell stage until approximately the 350-cell stage, with the segmentation and tracking results (surface renderings with arbitrary colors) overlaid on the raw image data (volume renderings). In this case, a level-set based model evolution approach was used for segmentation and tracking, modified from Dzyubachyk *et al.* (2010a). The bottom graph shows the lineage tree automatically derived from the tracking results, with the horizontal guidelines (red, dashed) corresponding to the four time points.

in the case of particle tracking, the available information to resolve potential ambiguities in the matching process is much more limited (often the particles all have similar appearance). In addition, particles may disappear, (re)appear, split, and merge. More consistent results can be achieved by using global rather than local linking strategies. Examples include spatio-temporal tracing (Bonneau *et al.*, 2005) and graph-based optimization approaches (Jaqaman *et al.*, 2008; Sbalzarini and Koumoutsakos, 2005). Alternatively, various Bayesian estimation approaches have been explored in recent years (Genovesio *et al.*, 2006; Godinez *et al.*, 2009; Smal *et al.*, 2008), with promising results (see Fig. 9.3 for an example).

3. Tracking Tools

Computational approaches to cell and particle tracking as described in the previous section are interesting in their own right but have no value to practitioners in the field unless they are implemented and released in the

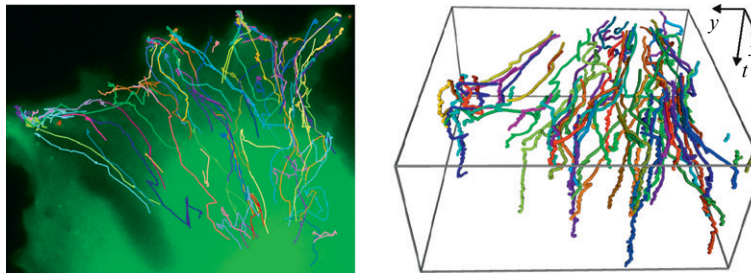

Figure 9.3 Particle tracking for studying vesicle dynamics. The left image shows the last frame of a 2D + *t* fluorescence microscopy image sequence of vesicles moving in the cytoplasm, with the detection and tracking results overlaid (arbitrarily colored trajectories). The results, adapted from Smal *et al.* (2008), were obtained using a tracking algorithm based on a Bayesian estimation framework, implemented by particle filtering. On the right, the trajectories are alternatively presented in a spatiotemporal rendering.

form of user-friendly software tools. Fortunately, there is an increasing tendency among computer scientists, spurred by various open source and reproducible research movements, to go the extra mile and develop such tools. Table 9.1 lists 30 currently available tools for cell and/or particle tracking, their main features, and where to find more detailed information about them. Here, we briefly comment on common aspects.

3.1. Cell tracking tools

The general assumption made by most cell tracking tools is that the cells can be modeled as bright regions against a darker background (the fluorescence microscopy scenario). If this is not the case, or if the images are too noisy, it is necessary to apply suitable filters to match this assumption. Most commercial tracking tools (such as Volocity, ImarisTrack, MetaMorph, Image-Pro Plus), as well as more general purpose open-source software packages (CellProfiler, FARSIGHT, ICY, and ImageJ/Fiji), offer ample functionality for image preprocessing.

Virtually all cell tracking tools are capable of tracking multiple cells and allow the user to compute basic dynamics parameters from the resulting trajectories. Few tools (such as StarryNite) are designed specifically for the study of embryogenesis, which requires not only segmentation and tracking of individual cells but also accurate handling of all cell divisions and the reconstruction of the complete cell lineage tree. Several freeware tools (such as AceTree (Boyle *et al.*, 2006; Murray *et al.*, 2006), and ALES (Braun *et al.*, 2003), not listed in the table) are available for the visualization, curation, and analysis of the cell lineages.

Table 9.1 Available tracking tools

Name	Available	Platform	Source	Cell	Particle	Multiple	Dimensions	Automation	Author of reference	Website
Braincells	Free	Win		√		√	2D	Manual	Gabor Ivancsy	http://pearl.elte.hu/~kyd
CellProfiler	Free	Win/Lin/Mac	√	√	√	√	2D	Auto	Carpenter *et al.* (2006)	http://www.cellprofiler.org/
CellTrack	Free	Win	√	√		√	2D	Auto	Sacan *et al.* (2008)	http://db.cse.ohio-state.edu/CellTrack/
CellTracker	Free	Win		√		√	2D	Semi	Shen *et al.* (2006)	http://go.warwick.ac.uk/bretschneider/celltracker/
ClusterTrack	Free	Matlab	√		√	√	2D	Auto	Matov *et al.* (2010)	http://lccb.hms.harvard.edu/software.html
DcellIQ	Free	Matlab	√	√		√	2D	Auto	Li *et al.* (2010)	http://www.cbi-tmhs.org/Dcelliq/
DIAS	Paid	Win/Mac		√		√	3D	Auto	Wessels *et al.* (2006)	http://keck.biology.uiowa.edu/
DiaTrack	Paid	Win		√	√	√	3D	Auto	Semassopht, Switzerland	http://ww.semasopht.com/
DYNAMIK	Free	Matlab	√	√		√	2D	Auto	Mosig *et al.* (2009)	http://www.picb.ac.cn/sysbio/DYNAMIK/
FARSIGHT	Free	Win/Lin/Mac	√	√		√	3D	Auto	Bjornsson *et al.* (2008)	http://www.farsight-toolkit.org/
ICY	Free	Java	√	√	√	√	3D	Auto	de Chaumont *et al.* (2011)	http://icy.bioimagenalysis.org/
Image-Pro Plus	Paid	Win		√	√	√	3D	Auto	Media Cybernetics, USA	http://www.mediacy.com/index.aspx?page=IPP
ImarisTrack	Paid	Win/Mac		√	√	√	3D	Auto	Bitplane, Switzerland	http://www.bitplane.com/go/products/imaristrack

(*Continued*)

Table 9.1 (*Continued*)

Name	Available	Platform	Source	Cell	Particle	Multiple	Dimensions	Automation	Author of reference	Website
LevelSetTracker	Free	Matlab	\	\		\	3D	Auto	Dzyubachyk *et al.* (2010b)	http://celmia.bigr.nl/
LineageTracker	Free	ImageJ		\		\	2D	Auto	Till Bretschneider	http://go.warwick.ac.uk/bretschneider/lineagetracker/
ManualTracking	Free	ImageJ	\		\	\	3D	Manual	Fabrice Cordelières	http://rsb.info.nih.gov/ij/plugins/track/track.thtml
MetaMorph	Paid	Win		\	\	\	3D	Auto	Molecular Devices, USA	http://www.moleculardevices.com/Products/Software.html
Mtrack2	Free	ImageJ	\		\	\	2D	Auto	Nico Stuurman	http://valelab.ucsf.edu/~nico/IJplugins/MTrack2.html
MTrackJ	Free	ImageJ	\		\	\	3D	Manual	Erik Meijering	http://www.imagescience.org/meijering/software/mtrackj/
Octane	Free	ImageJ	\		\	\	2D	Auto	Ji Yu lab	http://www.ccam.uchc.edu/yu/Software.html
Oko-Vision	Paid	Win		\		\	2D	Semi	Okolab, Italy	http://www.oko-lab.com/cell_tracking.page
ParticleTracker	Free	ImageJ	\		\	\	3D	Auto	Sbalzarini and Koumoutsakos (2005)	http://weeman.inf.ethz.ch/ParticleTracker/
plusTipTracker	Free	Matlab	\		\	\	2D	Auto	Danuser lab	http://lccb.hms.harvard.edu/software.html

QuimP	Free	ImageJ		\			2D	Auto	Bosgraaf *et al.* (2009)	http://go.warwick.ac.uk/bretschneider/quimp/
SpotTracker	Free	ImageJ			\		2D	Auto	Sage *et al.* (2005)	http://www.bigwww.epfl.ch/sage/soft/spottracker
StarryNite	Free	Win/Lin		\		\	3D	Auto	Murray *et al.* (2006)	http://westerston.gs.washington.edu/
TIKAL	Request	Win/Lin			\	\	3D	Auto	Bacher *et al.* (2004)	http://ibios.dkfz.de/tbi/
TLA	Free	Matlab	\	\		\	2D	Auto	Kestler lab	http://www.informatik.uni-ulm.de/ni/staff/HKestler/tla/
u-track	Free	Matlab	\		\	\	2D	Auto	Jaqaman *et al.* (2008)	http://lccb.hms.harvard.edu/software.html
Volocity	Paid	Win/Mac		\	\	\	3D	Auto	Perkin Elmer, USA	http://cellularimaging.perkinelmer.com/products/volocity/demo/

The columns indicate (from left to right) the name of the tool, availability (Free = freeware, Paid = paid license code required or available as a paid service only, Request = freely available from the developers on request), the platform on which the tool runs (Java = runs on all platforms with Java installed, ImageJ = plugin for ImageJ and runs on all platforms with Java installed, Lin = distribution for Linux, Mac = distribution for Mac OS X, Matlab = runs on all platforms with Matlab installed, Win = distribution for Microsoft Windows), whether source code is available, whether it was developed primarily for cell tracking or for particle tracking, whether it can track multiple objects, the maximum spatial dimensionality per frame it can handle (2D image or 3D stack), the level of automation (Auto = automatic after initial parameter setting, Manual = requires continuous user input, Semi = partly automatic but requires user input), the author of the tool or a literature reference (with year) describing the tool, and finally the website where to find the tool.

3.2. Particle tracking tools

Similar to cell tracking, most particle tracking tools, too, assume the target objects (foci) to be significantly brighter than the local background, and prefiltering (noise reduction and deconvolution) of the images generally has a positive impact on their performance. In contrast with the mentioned commercial tools, many of which contain functionality for both cell tracking and particle tracking and are stand-alone applications, most freeware particle tracking tools are available either as a plugin of the widely used ImageJ/Fiji image analysis platform (MTrack2, Octane, ParticleTracker, SpotTracker) or as a Matlab module (plusTipTracker, u-track).

While all tracking tools generally perform well if the image data satisfy certain conditions (see the tips and tricks at the end of this chapter), experimental constraints often force these conditions to be violated, as a result of which automated tracking falls short or fails completely. Fixated on full automation, most tools offer very little functionality for manual trajectory inspection, curation, or creation. A tool specifically designed for this purpose is MTrackJ, an ImageJ/Fiji plugin, which at the time of writing has already been used in over a 100 scientific journal publications, testifying that fully automated tracking is still utopian in many situations.

4. Tracking Measures

The direct result of applying tracking tools is a sequence of coordinates indicating the position of each tracked object at each time point. While this is an essential step and a tremendous data reduction, from millions to billions of (mostly irrelevant) pixels to a few (or perhaps a few tens or hundreds of) thousands of coordinate values, by itself this does not lead to new insights. The final step to knowledge is the computation of biologically meaningful quantitative measures from these coordinates. Here, we distinguish four categories of measures, characterizing the motility, diffusivity, velocity, and morphology of the moving objects, respectively.

4.1. Motility measures

The first step toward quantitative analysis is to reconstruct the trajectories of the tracked objects from the measured coordinates. This problem of "connecting the dots" is practically always solved by linear interpolation, resulting in piecewise-linear trajectories, although higher-order interpolation schemes (in particular cubic splines) can be expected to yield (bio)physically more accurate representations. Given the trajectories, a variety of measures can be straightforwardly computed. The most obvious measures of motility

Table 9.2 Quantitative tracking measures commonly found in the literature

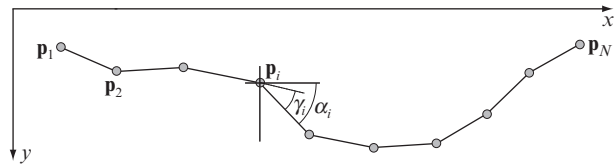

Measure	Definition
Total distance traveled	$d_{\text{tot}} = \sum_{i=1}^{N-1} d(\mathbf{p}_i, \mathbf{p}_{i+1})$
Net distance traveled	$d_{\text{net}} = d(\mathbf{p}_1, \mathbf{p}_N)$
Maximum distance traveled	$d_{\max} = \max_i d(\mathbf{p}_1, \mathbf{p}_i)$
Total trajectory time	$t_{\text{tot}} = (N-1)\Delta t$
Confinement ratio	$r_{\text{con}} = d_{\text{net}}/d_{\text{tot}}$
Instantaneous angle	$\alpha_i = \arctan(y_{i+1} - y_i)/(x_{i+1} - x_i)$
Directional change	$\gamma_i = \alpha_i - \alpha_{i-1}$
Instantaneous speed	$v_i = d(\mathbf{p}_i, \mathbf{p}_{i+1})/\Delta t$
Mean curvilinear speed	$\bar{v} = \frac{1}{N-1}\sum_{i=1}^{N-1} v_i$
Mean straight-line speed	$v_{\text{lin}} = d_{\text{net}}/t_{\text{tot}}$
Linearity of forward progression	$r_{\text{lin}} = v_{\text{lin}}/\bar{v}$
Mean squared displacement	$MSD(n) = \frac{1}{N-n}\sum_{i=1}^{N-n} d^2(\mathbf{p}_i, \mathbf{p}_{i+n})$

The drawing (top) shows a sample trajectory consisting of N points $\mathbf{p}_i = (x_i, y_i)$ and the table (bottom) defines the measures. The example is given for the 2D + t case but the measures can be extended straightforwardly to 3D + t. A constant frame rate is assumed with a time interval of Δt seconds between successive frames. The distance $d(\mathbf{p}_i, \mathbf{p}_j)$ between any two points $\mathbf{p}_i$ and $\mathbf{p}_j$ is usually taken to be the Euclidean norm $||\mathbf{p}_i - \mathbf{p}_j||$.

include (see Table 9.2 for definitions) the total trajectory length (the total distance traveled by the corresponding object), the distance between start and end point (the net distance traveled), the maximum distance to the start (or any other reference) point, and the confinement ratio (also referred to as the meandering index or the straightness index; Beltman *et al.*, 2009). Related measures, but for which varying definitions are found in the literature, include the chemotactic index and the McCutcheon index (Meijering *et al.*, 2008). Other obvious measures to compute are local orientations (with respect to the coordinate system or a reference point), directional change (turning angle; Beltman *et al.*, 2009; Soll, 1995), and the autocorrelation of the latter, which is indicative of directional persistence and process memory.

4.2. Diffusivity measures

A more sophisticated measure computable from a trajectory is the mean squared displacement (MSD). It is a function of time lag (see Table 9.2) and enables one to characterize the mode of motion of the corresponding object

by inspection of the resulting MSD-time curve (Qian *et al.*, 1991; Saxton and Jacobson, 1997). In the case of a pure random walk (such as Brownian motion of particles), the curve will be a straight line, given by $\mathrm{MSD}(t) = cDt$, with $c = 4$ in 2D and $c = 6$ in 3D, and where D denotes the so-called diffusion coefficient. If the motion is impeded by obstacles, the diffusion is anomalous, and characterized by $\mathrm{MSD}(t) = cDt^{\alpha}$ with $\alpha < 1$. An object whose motion is confined to some region will yield a curve that may be modeled as $\mathrm{MSD}(t) = R[1 - a_1 \exp(-a_2 cDt/R)]$, which converges to a maximum value R proportional to the size of the region, where a_1 and a_2 are positive constants related to the geometry of that region. The ultimate case of $R = 0$, corresponding to immobile objects, results in a curve that is zero everywhere. On the other hand, if there is directed motion (flow) in addition to diffusion, the curve behaves as $\mathrm{MSD}(t) = cDt + (vt)^2$, where v is the speed. Notice that the MSD is just the second-order moment of displacement. It may be helpful to compute other moment orders as well (Sbalzarini and Koumoutsakos, 2005).

4.3. Velocity measures

Other measures that can be easily derived from a trajectory are those concerning the rate of displacement. Instantaneous velocity, for example, is computed as the displacement from one frame to the next, divided by the time interval (Table 9.2). Notice that this quantity is a vector and its magnitude value is called speed, although in the literature the latter is also often referred to as velocity. A useful measure derived from instantaneous speed is the arrest coefficient (Beltman *et al.*, 2009), defined as the fraction of time that the object is pausing (having a speed less than some minimum value). The mean curvilinear speed is computed as the arithmetic mean of the instantaneous speeds. If the frame rate is constant, that is, if the time elapsed between any two successive frames in the image sequence is the same, this is equal to computing the ratio between the total distance traveled and the total trajectory time. Alternatively, if we use the net distance traveled, the ratio yields the mean straight-line speed. The ratio between the latter and the former speeds is a measure expressing the linearity of forward progression. Rather than taking grand averages, it is often useful to make speed histograms (Bahnson *et al.*, 2005; Qian *et al.*, 1991), as they give more insight into the statistics of the dynamics.

4.4. Morphology measures

In contrast with particle tracking, cell tracking algorithms usually record the entire cell shape at each time point, from which a position estimate is commonly derived by computing the centroid to which, in turn, the above mentioned measures can be applied. Having the full shape as a

function of time also allows for the computation of a host of measures characterizing the cell morphology (Bakal *et al.*, 2007; Soll, 1995). A distinction can be made here between measures of size and orientation versus measures of geometric complexity. Examples of the former in the case of 2D + *t* (and 3D + *t*) include the perimeter (surface area), area (volume), and the major and minor axes. Measures of (size and orientation invariant) complexity include circularity (sphericity), eccentricity (ellipticity), and convexity or concavity. More sophisticated analysis of morphology is possible by decomposing the shape in terms of Zernike polynomials or based on Fourier analysis, independent component analysis, or principal component analysis, the latter of which appears to be most suitable (see Pincus and Theriot (2007) for a thorough discussion).

5. Tips and Tricks

Concluding this chapter, we complement our discussion of tracking methods, tools, and measures with tips and tricks (including some serious warnings) concerning the imaging, tracking, and analysis. Since research goals, available equipment, and experimental conditions may vary widely, it is impossible to provide detailed protocols here. Nevertheless, the following general remarks should serve as a good basis for further consideration in designing cell and particle tracking experiments.

5.1. Imaging

- *Dimensionality*: The first thing to consider in preparing a time-lapse imaging experiment is whether to study the processes of interest in 2D or in 3D over time. If photobleaching and photodamage are to be minimized, or when dealing with very rapid motion of cells or particles, 3D + *t* imaging may simply be no option in view of the excess exposure and recording times required. However, biological processes naturally do take place in 3D + *t*, and it has been shown in various studies that 2D + *t* imaging and analysis may lead to different results (Meijering *et al.*, 2008). It is therefore important to verify one's assumptions.
- *Image quality*: One of the most critical factors affecting the performance of tracking tools is the signal-to-noise ratio (SNR) of the image data. Several studies (Carter *et al.*, 2005; Cheezum *et al.*, 2001; Smal *et al.*, 2010) have indicated that the accuracy, precision, and robustness of most particle detection and tracking methods drop rapidly for SNR < 4. Thus, in order to minimize tracking errors, the illumination settings should be such that at least this SNR is reached. Even though for cell tracking the SNR may be somewhat less critical than for particle tracking (as cells are

much larger and therefore more clearly visible), it is advisable to use a similar minimum level.

- *Frame rate*: Another critical imaging parameter to be tuned carefully is temporal resolution. It is obvious that in the case of directed motion, the lower the frame rate, the larger the distances traveled by the objects between frames, and thus the higher the chance of ambiguities in reconstructing trajectories. For cell tracking, as a rule of thumb, the frame rate should be chosen such that cells move less than their diameter from frame to frame (Zimmer *et al.*, 2006). For particle tracking, it has been suggested (Jaqaman and Danuser, 2009) that in order for the nearest-neighbor linking scheme (used in many tools) to perform well, the ratio (ρ) of the average frame-to-frame displacement and the average nearest-neighbor distance within frames should be $\rho \ll 0.5$.

5.2. Tracking

- *Preprocessing*: In live-cell imaging, the SNR (directly related to light exposure) is often deliberately minimized to avoid photobleaching and photodamage, while it ought to be maximized to ensure high tracking performance. This conflict of requirements may be resolved to some extent by processing the data prior to tracking. Noise reduction filters are widely available and in some tracking tools they are an integral part of the processing pipeline. Sophisticated filters have also been developed to transform transmitted light contrast images into pseudofluorescence images (Xiong and Iglesias, 2010), making them suitable for processing by tracking tools designed for fluorescence microscopy.
- *Tool selection*: As shown in this chapter, quite a number of tools already exist for cell and particle tracking, and it seems likely that more tools will become available in the near future. There is no single criterion to decide which of these is best for a given purpose, but Table 9.1 provides hints where to start looking. Commercial tools usually offer the most user-friendly interfaces and extensive functionality but may be prohibitively expensive. For many tracking and motion analysis tasks, freeware tools are often sufficient, and if source code is available, it is usually not difficult to tailor a tool to one's needs.
- *Verification*: The results of automated tracking are rarely perfect. The lower the SNR or the larger the number of objects, their density, motility, or similarity, the larger the risk of tracking errors. It is therefore advisable to visually inspect (a representative part of) the trajectories prior to analysis and, where necessary, to fix erroneous track initiation, termination, duplication, switching, splitting, and merging events (Beltman *et al.*, 2009). Unfortunately, most tools (especially freeware) lack flexible track-editing functionalities, and it may be helpful to use tools (such as MTrackJ) designed specifically for this purpose.

5.3. Analysis

- *Diffusivity*: Several warnings are in order when estimating diffusion coefficients from MSD-time curves (Meijering *et al.*, 2008). First, the 2D diffusion coefficient (computed from 2D tracking) is equal to the 3D coefficient only in isotropic media, where displacements in the three spatial dimensions are uncorrelated. Second, the shorter the trajectories, the higher the inaccuracy of diffusion estimates. Third, even for long trajectories, the inherent localization uncertainty may cause apparent subdiffusion patterns at short time scales. Finally, a trajectory may contain both diffusive and nondiffusive parts, which are obscured if the MSD is computed over the entire trajectory.
- *Velocity*: The estimation of velocities based on finite differencing of subsequent position estimates implicitly assumes linear motion from frame to frame. It is important to realize that this minimalist approach yields the lowest possible estimate and results in underestimation of the true velocities in cases where the dynamics is more complex. Another warning concerns velocity estimation of migrating cells. Commonly, this is based on the cell centroid position. However, in the case of considerable shape changes, the centroid position may show a much larger fluctuation and is no longer representative.
- *Aggregation*: A final issue to consider is how to aggregate the estimates of a parameter when tracking multiple objects. In principle, there are two approaches (Beltman *et al.*, 2009): object based or frame based, which may lead to different results, depending on the statistic. For example, when tracking objects consisting of two subpopulations (slow and fast moving), a histogram of the per-object mean speeds will reveal this, whereas the per-frame mean speed histogram does not. Conversely, frame-based analyses would allow the detection of different modes of motion (for a single object or a population of synchronized objects), which may go unnoticed with an object-based approach.

ACKNOWLEDGMENTS

The authors gratefully acknowledge financial support from the European Commission in the Seventh-Framework Programme (FP7 grant 201842) and from the Dutch Technology Foundation (STW) in the Smart Optics Systems Programme (SOS grant 10443).

REFERENCES

Bacher, C. P., Reichenzeller, M., Athale, C., Herrmann, H., and Eils, R. (2004). 4-D single particle tracking of synthetic and proteinaceous microspheres reveals preferential movement of nuclear particles along chromatin-poor tracks. *BMC Cell Biol.* **5,** 1–14.

Bahnson, A., Athanassiou, C., Koebler, D., Qian, L., Shun, T., Shields, D., Yu, H., Wang, H., Goff, J., Cheng, T., Houck, R., and Cowsert, L. (2005). Automated measurement of cell motility and proliferation. *BMC Cell Biol.* **6,** 19.

Bakal, C., Aach, J., Church, G., and Perrimon, N. (2007). Quantitative morphological signatures define local signaling networks regulating cell morphology. *Science* **316,** 1753–1756.

Beltman, J. B., Marée, A. F. M., and de Boer, R. J. (2009). Analysing immune cell migration. *Nat. Rev. Immunol.* **9,** 789–798.

Bjornsson, C. S., Lin, G., Al-Kofahi, Y., Narayanaswamy, A., Smith, K. L., Shain, W., and Roysam, B. (2008). Associative image analysis: A method for automated quantification of 3D multi-parameter images of brain tissue. *J. Neurosci. Methods* **170,** 165–178.

Bonneau, S., Dahan, M., and Cohen, L. D. (2005). Single quantum dot tracking based on perceptual grouping using minimal paths in a spatiotemporal volume. *IEEE Trans. Image Process.* **14,** 1384–1395.

Bosgraaf, L., van Haastert, P. J. M., and Bretschneider, T. (2009). Analysis of cell movement by simultaneous quantification of local membrane displacement and fluorescent intensities using Quimp2. *Cell Motil. Cytoskeleton* **66,** 156–165.

Boyle, T., Bao, Z., Murray, J. I., Araya, C. L., and Waterston, R. H. (2006). AceTree: A tool for visual analysis of Caenorhabditis elegans embryogenesis. *BMC Bioinformatics* **7,** 275.

Braun, V., Azevedo, R. B. R., Gumbel, M., Agapow, P. M., Leroi, A. M., and Meinzer, H. P. (2003). ALES: Cell lineage analysis and mapping of developmental events. *Bioinformatics* **19,** 851–858.

Carpenter, A. E., Jones, T. R., Lamprecht, M. R., Clarke, C., Kang, I. H., Friman, O., Guertin, D. A., Chang, J. H., Lindquist, R. A., Moffat, J., Golland, P., and Sabatini, D. M. (2006). CellProfiler: Image analysis software for identifying and quantifying cell phenotypes. *Genome Biol.* **7,** R100.

Carter, B. C., Shubeita, G. T., and Gross, S. P. (2005). Tracking single particles: A user-friendly quantitative evaluation. *Phys. Biol.* **2,** 60–72.

Cheezum, M. K., Walker, W. F., and Guilford, W. H. (2001). Quantitative comparison of algorithms for tracking single fluorescent particles. *Biophys. J.* **81,** 2378–2388.

de Chaumont, F., Dallongeville, S., and Olivo-Marin, J. C. (2011). ICY: A new open-source community image processing software. Proceedings of the IEEE International Symposium on Biomedical Imaging, pp. 234–237.

Dorn, J. F., Danuser, G., and Yang, G. (2008). Computational processing and analysis of dynamic fluorescence image data. *Methods Cell Biol.* **85,** 497–538.

Dzyubachyk, O., van Cappellen, W. A., Essers, J., Niessen, W. J., and Meijering, E. (2010a). Advanced level-set-based cell tracking in time-lapse fluorescence microscopy. *IEEE Trans. Med. Imaging* **29,** 852–867.

Dzyubachyk, O., Essers, J., Baldeyron, C., van Cappellen, W. A., Inagaki, A., Niessen, W. J., and Meijering, E. (2010b). Automated analysis of time-lapse fluorescence microscopy images: From live cell images to intracellular foci. *Bioinformatics* **26,** 2424–2430.

Genovesio, A., Liedl, T., Emiliani, V., Parak, W. J., Coppey-Moisan, M., and Olivo-Marin, J. C. (2006). Multiple particle tracking in 3-D+t microscopy: Method and application to the tracking of endocytosed quantum dots. *IEEE Trans. Image Process.* **15,** 1062–1070.

Godinez, W. J., Lampe, M., Wörz, S., Müller, B., Eils, R., and Rohr, K. (2009). Deterministic and probabilistic approaches for tracking virus particles in time-lapse fluorescence microscopy image sequences. *Med. Image Anal.* **13,** 325–342.

Jaqaman, K., and Danuser, G. (2009). Computational image analysis of cellular dynamics: A case study based on particle tracking. *Cold Spring Harb. Protoc.* **2009**, pdb.top65.

Jaqaman, K., Loerke, D., Mettlen, M., Kuwata, H., Grinstein, S., Schmid, S. L., and Danuser, G. (2008). Robust single-particle tracking in live-cell time-lapse sequences. *Nat. Methods* **5,** 695–702.

Li, F., Zhou, X., Ma, J., and Wong, S. T. C. (2010). Multiple nuclei tracking using integer programming for quantitative cancer cell cycle analysis. *IEEE Trans. Med. Imaging* **29,** 96–105.

Matov, A., Applegate, K., Kumar, P., Thoma, C., Krek, W., Danuser, G., and Wittmann, T. (2010). Analysis of microtubule dynamic instability using a plus-end growth marker. *Nat. Methods* **7,** 761–768.

Meijering, E., Smal, I., and Danuser, G. (2006). Tracking in molecular bioimaging. *IEEE Signal Process. Mag.* **23,** 46–53.

Meijering, E., Smal, I., Dzyubachyk, O., and Olivo-Marin, J. C. (2008). Time-lapse imaging. *In* "Microscope Image Processing," (Q. Wu, F. A. Merchant, and K. R. Castleman, eds.), pp. 401–440. Academic Press, Burlington, MA. pp. 401–440, Chapter 15.

Meijering, E., Dzyubachyk, O., Smal, I., and van Cappellen, W. A. (2009). Tracking in cell and developmental biology. *Semin. Cell Dev. Biol.* **20,** 894–902.

Mosig, A., Jäger, S., Wang, C., Nath, S., Ersoy, I., Palaniappan, K. P., and Chen, S. S. (2009). Tracking cells in life cell imaging videos using topological alignments. *Algorithms Mol. Biol.* **4,** 10.

Murray, J. I., Bao, Z., Boyle, T. J., and Waterston, R. H. (2006). The lineaging of fluorescently-labeled Caenorhabditis elegans embryos with StarryNite and AceTree. *Nat. Protoc.* **1,** 1468–1476.

Peng, H. (2008). Bioimage informatics: A new area of engineering biology. *Bioinformatics* **24,** 1827–1836.

Pincus, Z., and Theriot, J. A. (2007). Comparison of quantitative methods for cell-shape analysis. *J. Microsc.* **227,** 140–156.

Qian, H., Sheetz, M. P., and Elson, E. L. (1991). Single particle tracking: Analysis of diffusion and flow in two-dimensional systems. *Biophys. J.* **60,** 910–921.

Rittscher, J. (2010). Characterization of biological processes through automated image analysis. *Annu. Rev. Biomed. Eng.* **12,** 315–344.

Rohr, K., Godinez, W. J., Harder, N., Wörz, S., Mattes, J., Tvaruskó, W., and Eils, R. (2010). Tracking and quantitative analysis of dynamic movements of cells and particles. *Cold Spring Harb. Protoc.* **2010,** pdb.top80.

Sacan, A., Ferhatosmanoglu, H., and Coskun, H. (2008). Cell track: An open-source software for cell tracking and motility analysis. *Bioinformatics* **24,** 1647–1649.

Sage, D., Neumann, F. R., Hediger, F., Gasser, S. M., and Unser, M. (2005). Automatic tracking of individual fluorescence particles: Application to the study of chromosome dynamics. *IEEE Trans. Image Process.* **14,** 1372–1383.

Saxton, M. J., and Jacobson, K. (1997). Single-particle tracking: Applications to membrane dynamics. *Annu. Rev. Biophys. Biomol. Struct.* **26,** 373–399.

Sbalzarini, I. F., and Koumoutsakos, P. (2005). Feature point tracking and trajectory analysis for video imaging in cell biology. *J. Struct. Biol.* **151,** 182–195.

Shen, H., Nelson, G., Kennedy, S., Nelson, D., Johnson, J., Spiller, D., White, M. R. H., and Kell, D. B. (2006). Automatic tracking of biological cells and compartments using particle filters and active contours. *Chemometr. Intell. Lab. Syst.* **82,** 276–282.

Smal, I., Meijering, E., Draegestein, K., Galjart, N., Grigoriev, I., Akhmanova, A., van Royen, M. E., Houtsmuller, A. B., and Niessen, W. (2008). Multiple object tracking in molecular bioimaging by Rao-Blackwellized marginal particle filtering. *Med. Image Anal.* **12,** 764–777.

Smal, I., Loog, M., Niessen, W., and Meijering, E. (2010). Quantitative comparison of spot detection methods in fluorescence microscopy. *IEEE Trans. Med. Imaging* **29,** 282–301.

Soll, D. R. (1995). The use of computers in understanding how animal cells crawl. *Int. Rev. Cytol.* **163,** 43–104.

Swedlow, J. R., Goldberg, I. G., Eliceiri, K. W., and OME Consortium (2009). Bioimage informatics for experimental biology. *Annu. Rev. Biophys.* **38,** 327–346.

Tsien, R. Y. (2003). Imagining imaging's future. *Nat. Rev. Mol. Cell Biol.* **4,** S16–S21.

Vonesch, C., Aguet, F., Vonesch, J. L., and Unser, M. (2006). The colored revolution of bioimaging. *IEEE Signal Process. Mag.* **23,** 20–31.

Wessels, D., Kuhl, S., and Soll, D. R. (2006). Application of 2D and 3D DIAS to motion analysis of live cells in transmission and confocal microscopy imaging. *Methods Mol. Biol.* **346,** 261–279.

Xiong, Y., and Iglesias, P. A. (2010). Tools for analyzing cell shape changes during chemotaxis. *Integr. Biol.* **2,** 561–567.

Zimmer, C., Zhang, B., Dufour, A., Thébaud, A., Berlemont, S., Meas-Yedid, V., and Olivo-Marin, J. C. (2006). On the digital trail of mobile cells. *IEEE Signal Process. Mag.* **23,** 54–62.